Publication No. 02-187-254

ISOLATION AND CHARACTERIZATION OF RARE EARTH MINERAL PARTICLES IN FLORIDA PHOSPHATE ROCK BY DE RAPID SCAN RADIOGRAPHY AND HRXMT

Prepared by

UNIVERSITY OF UTAH
Salt Lake City, UT

under a grant sponsored by

August 2015

The Florida Industrial and Phosphate Research Institute (FIPR Institute) was created in 2010 by the Florida Legislature (Chapter 1004.346, Florida Statutes) as part of the University of South Florida Polytechnic. The FIPR Institute superseded the Florida Institute of Phosphate Research established in 1978 but retained and expanded its mission. In April 2012 the statute was amended by the Florida Legislature, transferring the Institute to the Florida Polytechnic University as of July 1, 2012. The FIPR Institute is empowered to expend funds appropriated to the University from the Phosphate Research Trust Fund. It is also empowered to seek outside funding in order to perform research and develop methods for better and more efficient processes and practices for commercial and industrial activities, including, but not limited to, mitigating the health and environmental effects of such activities as well as developing and evaluating alternatives and technologies. Within its phosphate research program, the Institute has targeted areas of research responsibility. These are: establish methods for better and more efficient practices for phosphate mining and processing; conduct or contract for studies on the environmental and health effects of phosphate mining and reclamation; conduct or contract for studies of reclamation alternatives and wetlands reclamation; conduct or contract for studies of phosphatic clay and phosphogypsum disposal and utilization as a part of phosphate mining and processing; and provide the public with access to the results of its activities and maintain a public library related to the institute's activities.

The FIPR Institute is located in Polk County, in the heart of the Central Florida phosphate district. The Institute seeks to serve as an information center on phosphate-related topics and welcomes information requests made in person, or by mail, email, fax, or telephone.

Florida Industrial and Phosphate Research Institute
1855 West Main Street
Bartow, Florida 33830
(863) 534-7160
Fax: (863) 534-7165
http://www.fipr.state.fl.us

ISOLATION AND CHARACTERIZATION OF RARE EARTH MINERAL PARTICLES IN FLORIDA PHOSPHATE ROCK BY DE RAPID SCAN RADIOGRAPHY AND HRXMT

FINAL REPORT

Jan D. Miller
Principal Investigator

and

Team Members
C.L. Lin and Raquel Crossman

Metallurgical Engineering Department
College of Mines and Earth Sciences
UNIVERSITY OF UTAH
Salt Lake City, UT 84112

Prepared for

FLORIDA INDUSTRIAL AND PHOSPHATE RESEARCH INSTITUTE
1855 West Main Street
Bartow, FL 33830 USA

Project Manager: Dr. Patrick Zhang
FIPR Project Number: 12-02-187

August 2015

DISCLAIMER

The contents of this report are reproduced herein as received from the contractor. The report may have been edited as to format in conformance with the FIPR Institute *Style Manual*.

The opinions, findings and conclusions expressed herein are not necessarily those of the Florida Industrial and Phosphate Research Institute or its predecessor, the Florida Institute of Phosphate Research, nor does mention of company names or products constitute endorsement by the Florida Industrial and Phosphate Research Institute.

PERSPECTIVE

Patrick Zhang, Research Director - Beneficiation & Mining

Rare earth elements (REE) are critical to national security from the Department of Defense to Homeland Security; to the development of green energy as used in hybrid cars and wind turbines; and to advancement of various high-tech fields such as computing and internet technology. They are also vital to many traditional industries such as petroleum refining and glass polishing. The U.S. faces a critical shortage of these elements. The demand for these elements cannot be presently met directly from rare earths mines, and alternative sources must be found to fill this need. Florida phosphate could be one of the alternative sources. FIPR recently conducted a characterization study of REE in Florida phosphate, and found appreciable amounts of REE in currently mined ore, with one flotation concentrate analyzing above 900 ppm of total REE. In Florida, approximately 30,000 tons of rare earth elements are discarded annually in various phosphate mining and processing streams, while the current U.S. demand for REE is less than 15,000 tons per year.

The high potential to meet the entire U.S. demand by recovering REE from Florida phosphate prompted FIPR to team up with the Oak Ridge National Laboratory (ORNL) in applying for a $120 million funding award by the U.S. Department of Energy (DOE) to establish a new Energy Innovation Hub on critical materials. FIPR and ORNL decided to join the Critical Materials Institute (CMI), led by the Ames Laboratory. CMI succeeded in securing the DOE funding in early 2013, and FIPR was awarded a five-year contract to work on the project *Recovery of REEs and Uranium from Phosphate Ore Processing*. This University of Utah study on isolation and characterization of rare earths mineral particles in Florida phosphate rock was funded because it complements the FIPR efforts under the CMI project.

Since REE-containing minerals exist in phosphate processing streams within ppm ranges, the identification and quantification of these minerals are nearly impossible using traditional X-ray diffraction and microscopic methods. This project was designed to isolate and analyze rare earths-containing minerals in phosphate mining and processing streams using the most advanced mineral characterization techniques, high-resolution X-ray micro tomography (HRXMT) and dual-energy (DE) rapid scan radiography. This type of information is critical to developing methods for extracting rare earth elements from phosphate.

Results from this project show that DE radiography followed by HRXMT scanning is an effective and efficient method for resource identification in general, and is particularly well-suited for REE mineral identification. One major REE mineral identified in all samples is monazite, which may be one of the reasons why a majority of the REE in phosphate rock reports to phosphogypsum during the acidulation process, since monazite is difficult to dissolve at low temperatures. One of the remaining challenges in characterizing REE minerals in phosphate is to analyze the amount of REE as calcium substitution in phosphate crystals.

ABSTRACT

Due to the national dependence on China to supply nearly all the demand for rare earth minerals, a project was proposed to investigate the RE minerals contained in Florida's phosphate rock. Because traditional methods for resource identification often overlook trace amounts of minerals, dual-energy (DE) radiography followed by high-resolution X-ray microtomography (HRXMT) was used to characterize the rare earth minerals contained within Florida mining samples and to give liberation details. Three sample streams, shaking table concentrate, acid plant feed, and phosphogypsum, were separated into three size classes: >106 μm, 75-106 μm, and 53-75 μm. DE radiographs were taken at two energy levels and the ratio calculated. The images were thresholded to show only potential rare earth particles and then those particles were removed to prepare HRXMT samples. The samples were digitally reconstructed and the concentration of rare earth particles found using digital processing software. The overall concentrations for the three size classes were found to be 2157 ppm in the shaking table concentrate, 104 ppm in the acid plant feed, and 284 ppm in the phosphogypsum, respectively. Based on the degree of liberation, the best particle size to find fully liberated monazite particles is 75-106 μm.

TABLE OF CONTENTS

LIST OF FIGURES

Figure **Page**

EXECUTIVE SUMMARY

The purpose of this project was to isolate and characterize phosphate rare earth (RE) particles from concentrate and tailing samples provided by the Florida Industrial and Phosphate Research Institute. This was done by using dual-energy (DE) rapid scan radiography to first identify potential RE particles, followed by a more detailed quantified liberation analysis by high-resolution X-ray microtomography (HRXMT). The Xradia Micro XCT400 was used for both DE Radiography and for HRXMT.

While characterization is usually accomplished using methods such as X-ray fluorescence (XRF), X-ray diffraction (XRD), and scanning electron microscopy (SEM) techniques, the sample must often be altered or destroyed during sample preparation and liberation is always overestimated because they only scan two dimensions and estimate the third. HRXMT offers full 3D imaging and analysis with simple sample preparation and no sample destruction. However, the time required for HRXMT scanning and analysis is usually several hours and can be as long as half a day. By scanning first with DE radiography, scanning time is significantly reduced by providing semi-quantitative information in a fraction of the time required for HRXMT.

Using this method is particularly useful for identifying RE particles because of the concentration levels in which they are usually found. As trace minerals, they are generally found only on a parts per million (ppm) scale. This means that potentially millions of particles must be examined in order to provide a statistically reliable accuracy. Additionally, other methods often overlook trace particles such as RE minerals in their analysis due to their small concentration. Therefore, DE radiography followed by HRXMT was used to isolate and characterize RE particles from the shaking table concentrate, acid plant feed, and phosphogypsum samples provided.

As initial preparation, the samples were first separated into size classes by dry and wet separation using sieves of size 140 mesh (106 μm), 200 mesh (75 μm), and 270 mesh (53 μm). DE radiography samples were prepared by applying double-sided sticky tape to a 3" × 1" glass slide. Particles from the samples were spread onto the tape and a second slide attached using regular tape. Three slides from each size classification (>106 μm, 75-106 μm, and 53-75 μm) for each sample were prepared, for a total of 27 slides.

Before scans were completed, a calibration for both DE radiography and HRXMT was necessary. To do this, a heavy-density sample was taken for an initial XRD analysis. From this, it was discovered that the samples contained monazite, zircon, and apatite. Using XMuDat, the relationship between the linear attenuation coefficient and energy level was mapped for each of these minerals, and based on the resulting graphs it was determined that 70 kV was the best energy level for them. Pure samples of each of these minerals were scanned using HRXMT in order to create a mineral standard to be used during HRXMT reconstruction. Additionally, aluminum, copper, and lead were scanned using DE radiography in order to calculate the DE radiography coefficients k_1, k_2, k_3, and

k_4 with the parameter, p, set at 3.8. The resulting values were $k_1 = -8.97 \cdot 10^{11}$, $k_2 = 7.95 \cdot 10^{11}$, $k_3 = 1.88 \cdot 10^{6}$ and $k_4 = -1.16 \cdot 10^{6}$.

Scans were completed using an Xradia MicroXCT-400 machine. For DE radiography, a 4 × 10 grid was created, separating each slide into 40 sections. Each section was scanned at two energy levels, 80 kV and 140 kV. Additionally, a reference image was taken for each slide at both energy levels, which normalizes the image to be a percentage of the emission X-ray. After each scan was completed, they were imported to Matlab and the ratio of the low-energy image to the high-energy image, also known as the relative reflex, was calculated at each pixel. A threshold of 0.70 was then applied to each image in order to identify which particles were potential RE particles.

The thresholded images were then used to identify which particles to remove for HRXMT sample preparation. These samples were prepared by taking a 5 mm syringe secured on a toothpick and placing the particles between two syringe plungers. This allowed the particles to be secured within the syringe so no movement occurred during scanning. Three HRXMT samples were prepared, one for each sample stream, and potential RE particles from each slide were separated from each other using a piece of circular paper in order to keep the particles separated by size.

HRXMT samples were scanned using the same Xradia MicroXCT-400 machine. The samples were rotated a full 360° while taking 1000 image projections at the 70 kV energy level. The samples were then reconstructed as a 3D digital image using Xradia's attached software, XMReconstructor. This allowed the samples to be viewed as 2D slices of the 3D sample, or as a full 3D image that could be rotated to view more thoroughly.

Using digital image processing software Drishti, the 3D images were rendered, then thresholded to allow only the particles of a certain attenuation to be viewed. This allowed for the size distribution of RE particles to be seen based on the HRXMT sample preparation from DE slides. In the shaking table concentrate, the majority of the RE particles were found in the size class of 75-106 μm. A similar, but not as concentrated, grouping was found in the phosphogypsum sample, but RE particles were also found in the larger and smaller size class. There is no such concentration in the acid plant feed, and the overall concentration for this sample was much smaller than the other samples. After this visual analysis was completed, digital image processing software ImageJ was used to count the number of particles past a certain threshold. Accordingly, there were 660 RE particles in the shaking table concentrate, 32 in the acid plant feed, and 87 in the phosphogypsum. This calculates to the concentrations of 2157 ppm in the shaking table concentrate, 104 ppm in the acid plant feed, and 284 ppm in the phosphogypsum.

Based on these results, it is recommended that DE radiography, with follow-up confirmation by HRXMT, be used in the future to accurately and rapid identify RE particles and the degree of liberation for each size class.

INTRODUCTION

Resource evaluation and characterization is necessary for the development of process strategies for the recovery of rare earth (RE) minerals from phosphate rock. RE oxides are used to produce a number of things, including automotive catalytic converters, phosphors in color television and flat panel displays (i.e., cell phones, laptops, etc.), permanent magnets, and a number of defense devices such as engines, guidance systems, satellites, and communication systems.

In the U.S., between 2002 and 2010, about 5 to 11 kilotons of RE oxides were consumed each year, the majority of which were imported. Globally, it is estimated that the demand for RE elements will reach 160,000 metric tons by 2016. About 97% of the world's RE production comes from China, making the global supply chain almost entirely dependent on China and subjective to its political and economic disputes and whims. In addition to this, with increasing global demands it is also predicted that there will be a shortage of RE elements produced (Humphries 2013).

In order to change this and satisfy the demands for RE production in the U.S., it was decided to investigate the recovery of RE minerals from phosphate rock, particularly those distributed in Florida phosphate rock. RE minerals make up about 0.01 to 0.1% of apatite mineral concentration, averaging about 0.5% RE oxides. Because about 170 million tons of phosphate rock are processed annually, this can amount to a significant RE oxide production (Zhang 2012).

Traditional analytical methods such as XRD, XRF, and SEM have limitations for trace mineral identification. Also, these analytical techniques are limited with respect to liberation analysis. For example, automated SEM analysis of polished sections provides 2D information and so always overestimates liberation. In addition, sample preparation for these methods often involves altering or completely destroying the sample. To prevent these errors and preserve the sample, 3D liberation analysis by high-resolution X-ray microtomography (HRXMT) is highly recommended. However, the time for complete analysis is lengthy, from several hours to half a day depending on the desired voxel resolution (5 to 1 microns, respectively). Because RE mineral particles are present in phosphate rock at the ppm scale, potentially millions of particles must be examined in order to provide statistically reliable accuracy and confidence in the characterization analysis. To scan that many particles with HRXMT can take a significant amount of time. To reduce this time, dual-energy (DE) radiography can be used to provide semi-quantitative information in a fraction of the time. The potential RE particles can then be scanned by HRXMT to provide full analysis.

Therefore, a one-year research program was completed to demonstrate the ability to isolate and characterize RE mineral particles from Florida phosphate rock by DE radiography followed by a more detailed liberation analysis in 3D by HRXMT.

METHODOLOGY

TASK 1: SAMPLE COLLECTION CHARACTERIZATION

Particle Size Separation

The first two samples received from FIPR were the shaking table concentrate and the acid plant feed. There was about a kilogram of each sample that needed to be separated into size classes. To do this, three sieves were chosen: 140 mesh (106 μm), 200 mesh (75 μm), and 270 mesh (53 μm). A vibrating sieve shaker was used to do this separation of each sample, first as dry sieving, then again as a wet sieving for thorough and effective separation. Four size classes were prepared: >106 microns, 75-106 microns, 53-75 microns, and <53 microns. Because the last class was so small, no further testing was done on this portion, which left three size classes to be examined for each sample.

Because of the length of time required for the double separation of dry sieving followed by wet sieving, when the third sample (phosphogypsum) arrived, a different method was applied. Coning and quartering was used instead of dry separation, reducing the bulk sample in content from approximately one kilogram to a bit more than 100 grams. The 100 gram sample was then separated into size classes using the same wet sieving on the vibrating sieve shaker as was used for the other two samples.

Sample Collection Characterization

Before proceeding to DE radiography and HRXMT, it was necessary to get an idea of what was present in the samples. A chemical analysis of the acid plant feed was provided, as can be seen in Table 1, and an approximate estimation for shaking table concentrate in Table 2. To get a more exact concentration for the shaking table concentrate, a portion of the >106 microns sample was further separated using gravity separation by hand panning. The heavy particles were separated out from the lighter ones and taken for X-ray diffraction (XRD) and HRXMT. The results from the XRD are shown in Figure 1 and the results from the HRXMT are shown in Figure 2. HRXMT scans were done using the calibration procedure discussed in Task 2. As can be seen, the minerals identified in the sample were zircon ($ZrSiO_4$), apatite ($Ca_5(PO_4)_3(OH,F,Cl)$), and monazite ($(Ce,La)PO_4$).

Table 1. Chemical Analysis of Provided Acid Plant Feed.

P_2O_5 (ICP)	P_2O_5 (Lachat)	Insol	MgO	Fe_2O_3	Al_2O_3	CaO
26.46	27.36	15.84	0.50	1.19	1.19	38.84
Pr (ppm)	Eu (ppm)	Tb (ppm)	Dy (ppm)	Ho (ppm)	Er (ppm)	Tm (ppm)
7.92	3.48	2.17	13.81	3.25	9.62	1.22
Yb (ppm)	Lu (ppm)	Sc (ppm)	Gd (ppm)	Sm (ppm)	Th (ppm)	U (ppm)
8.69	1.34	4.90	16.46	12.04	9.15	87.77
Ce (ppm)	Y (ppm)	La (ppm)	Nd (ppm)			
131.16	132.06	77.58	85.26			

Table 2. Estimated Chemical Analysis of Provided Shaking Table Concentrate.

P_2O_5 (ICP)	P_2O_5 (Lachat)	Insol	MgO	Fe_2O_3	Al_2O_3	CaO
6-9	6-9	70-80	0.03-0.08	0.29-0.9	0.28-0.8	8-15
Pr (ppm)	Eu (ppm)	Tb (ppm)	Dy (ppm)	Ho (ppm)	Er (ppm)	Tm (ppm)
10-16	2-3	0.5-0.7	5.0-7.5	2-3	6-11	1.0-1.5
Yb (ppm)	Lu (ppm)	Sc (ppm)	Gd (ppm)	Sm (ppm)	Th (ppm)	U (ppm)
4.0-6.0	0.10-0.15	3.0-4.5	8-11	10-18	8.0-10.0	30-50
Ce (ppm)	Y (ppm)	La (ppm)	Nd (ppm)			
130-150	70-100	60-90	80-110			

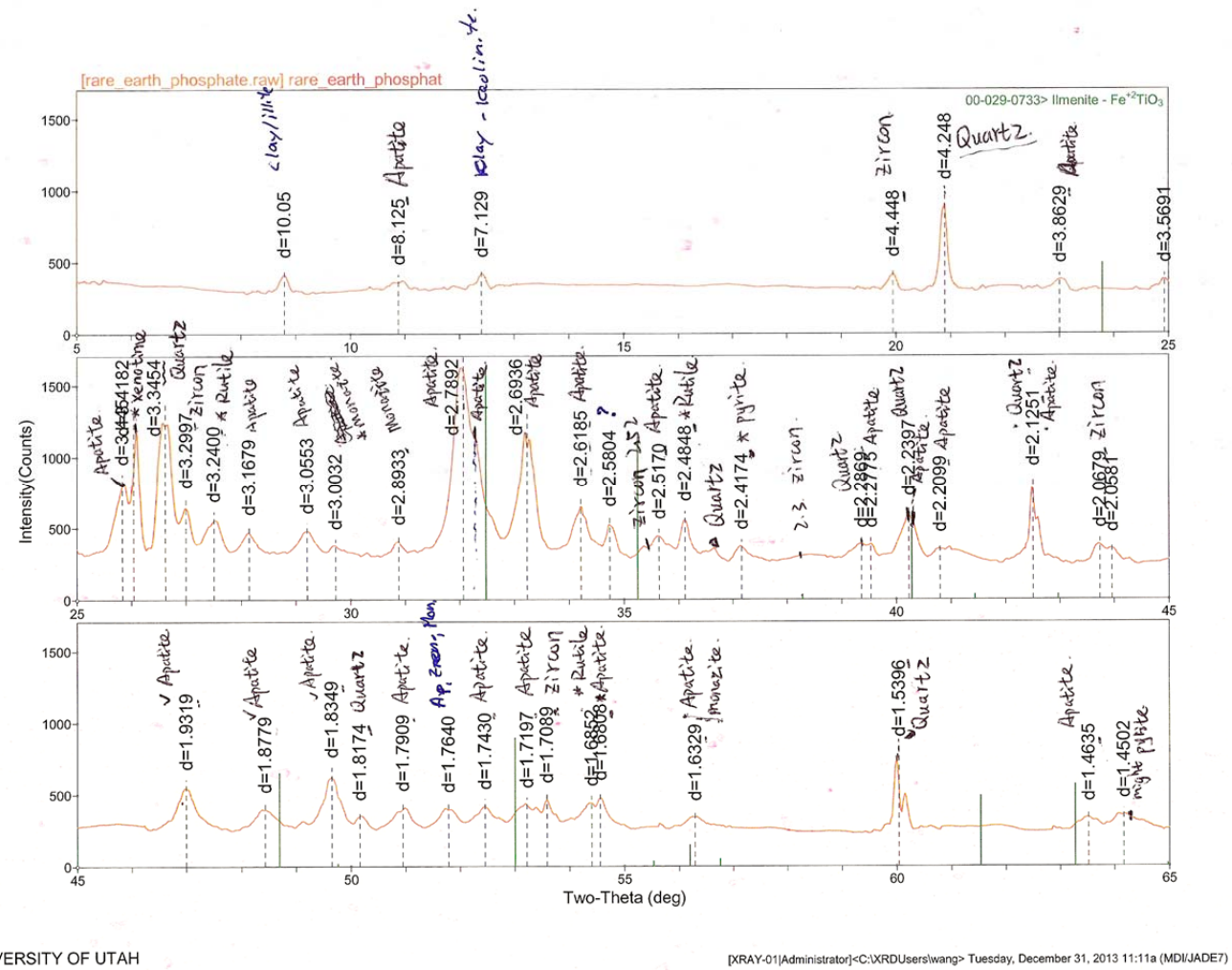

Figure 1. Results from XRD Analysis of Heavy Particles from Shaking Table Concentrate.

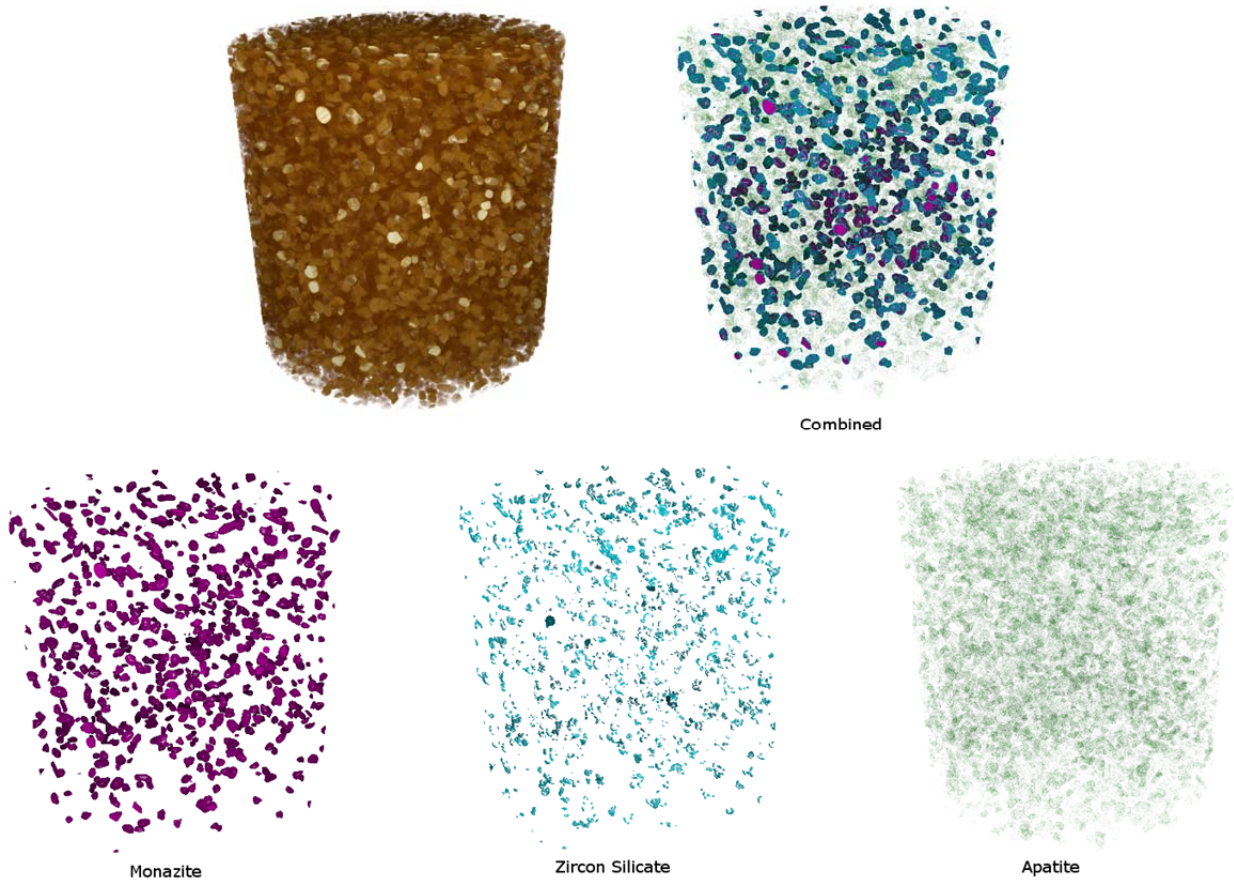

Figure 2. Reconstructed 3D Rendered Images from HRXMT Scans of the High-Density Fraction of Shaking Table Concentrate Containing Monazite, Zircon, Apatite, Etc.

TASK 2: CALIBRATION

Dual-Energy Calibration

Theory

X-ray radiography can be used to produce a two-dimensional map of X-ray attenuation coefficients of irradiated ore samples. A monochromatic X-ray of energy E and incident photon flux density or intensity (number of photons/unit time and area), I_0, on passing through local material that absorbs X-ray photons and having a thickness x, will have an emerging photon intensity I given by:

$$I = I_0 \cdot \exp\left(-\mu(\rho, Z, E) \cdot x\right) \tag{1}$$

where μ is the linear attenuation coefficient, depending on density, ρ; atomic number, Z; and the energy of the X-ray beam, E. For two energy levels (low and high), Equation 1 can be written as

$$I(E_i) = I_0(E_i) \cdot \exp\left(-\mu(\rho, Z, E_i) \cdot x\right) \quad i = Low, High \tag{2}$$

Differentiation of mineral phases within the sample is complicated because the linear attenuation coefficient, μ, at each voxel depends directly on the electron density, the effective atomic number, Z_{eff}, of the material (composition) comprising the sample, and the energy of the X-ray beam, E. A simplified equation that illustrates the approximate relationship among these quantities is

$$\mu(E_i) = \rho[\alpha(E_i) + \beta(E_i) Z^{\,p}] \tag{3}$$

where the functions $\alpha(E)$ and $\beta(E)$ define the energy dependence of Compton and photoelectric effects, respectively.

Effective Atomic Number

The effective atomic number is simplified as Z_{eff} and the reflex ($R(E_i)$) is defined as:

$$R(E_i) = R_i = \ln(I_{0,i} / I_0) \tag{4}$$

at a specific energy level E_i. Then, Equations 2 and 3 can be combined as:

$$R(E_i)/\rho x = \mu_m \equiv [\alpha_i + \beta_i Z^p]Z \tag{5}$$

where $\mu_m = \mu/\rho$ is the mass attenuation coefficient. Based on the operating energy range (40 kV to 150 kV for the HRXMT), the dual-energy radiography technique involves both the Compton and photoelectric effects with $p \approx 3.8$ for this study.

The effective atomic number of an unknown material can be calculated by three known materials and measurements in a specific energy range using the dual-energy radiographic technique (Naydenov and others 2003). In this case, the relative reflex of two radiographs, $X = R_1/R_2$, plays the principal role in the estimation of the effective atomic number, Z_{eff}, of an unknown material. From Equation 5,

$$X \equiv R(E_1)/R(E_2) = \mu_m(E_1)/\mu_m(E2) = \mu(E_1)/\mu(E_2) \tag{6}$$

Therefore, X depends only on the effective atomic number and does not depend on the geometry (thickness, x) nor the density of the material (ρ). In this way, Z_{eff} of an unknown material can be estimated based on dual-energy radiography.

$$Z_{eff} \equiv ((k_1 \cdot X + k_2)/(k_1 \cdot X + k_2))^{1/p} \tag{7}$$

where the relative reflex, $X = R_1/R_2$, from two radiographs at different energy levels, and the coefficients k_1, k_2, k_3 and k_4 are reconstructed from the relative reflexes of three known materials, as described by the following equations:

$$\begin{aligned}
k_1 &= Z_1^p Z_2^p (X_1 - X_2) - Z_1^p Z_3^p (X_1 - X_3) + Z_2^p Z_3^p (X_2 - X_3) \\
k_2 &= X_1 X_2 Z_3^p (Z_1^p - Z_2^p) - X_1 X_3 Z_2^p (Z_1^p - Z_3^p) + X_2 X_3 Z_1^p (Z_2^p - Z_3^p) \\
k_3 &= X_1 (Z_2^p - Z_3^p) - X_2 (Z_1^p - Z_3^p) + X_3 (Z_1^p - Z_2^p) \\
k_4 &= X_1 X_2 (Z_1^p - Z_2^p) - X_1 X_3 (Z_1^p - Z_3^p) + X_2 X_3 (Z_2^p - Z_3^p)
\end{aligned} \tag{8}$$

where X_1, X_2 and X_3 are the relative reflexes of three known materials using the dual-energy method; Z_1, Z_2 and Z_3 are their effective atomic numbers.

Generally, this method provides the capability to calculate the effective atomic number of an unknown material using the dual-energy method. The dual-energy method works well as long as the energy range for each measured element does not involve the K-edge effect. With the effective atomic number and mineralogy of the sample, the unknown material can be characterized.

It should be noted that the theory of DE radiography and the corresponding calculations are based on a monochromatic power source. If the source is polychromatic instead, as is the case for this project, the method will have inevitable errors. The method may still be used, but the possibility of error must be taken into account. It is because of

this that DE radiography cannot be used for absolute mineral identification and can only be used semi-quantitatively.

Materials and Methods

Plastic plates, 3" × 1", and double-sided sticky tape were used to prepare the samples for DE radiography. Pure samples were placed on double-sided sticky tape, which was attached to a plastic plate, and then were stabilized with a second plate. For this case, two types of samples were prepared for mineral identification, which are shown in Figure 3. The image on the left shows the first sample with minerals used for calibration and the image on the right shows the second sample with minerals used for calibration verification. Table 3 shows more detailed information about the minerals used for verification.

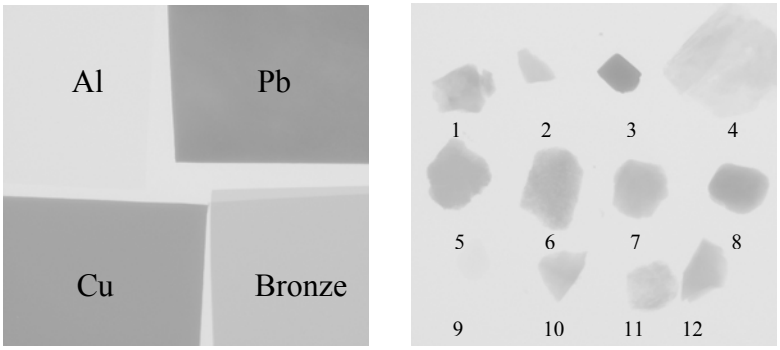

Figure 3. Radiographs of the Pure Reference Minerals and Minerals in Cu-Mo Flotation Tailing for DE Calibration.

Table 3. Detailed Information for Main Minerals in Cu-Mo Flotation Tailing.

	Mineral		Effective Atomic Number, Z_{actual}	Density, g/cm^3
	Name	Formula		
1	Molybdenite	MoS_2	36.87	4.6-4.7
2	Galena	PbS_2	78.96	7.2-7.6
3	Chalcopyrite	$CuFeS_2$	25.00	4.1-4.3
4	Bornite	Cu_5FeS_4	26.58	4.9-5.3
5	Barite	$BaSO_4$	48.73	4.3-5.0
6	Malachite	$Cu_3(CO_3)_2(OH)_2$	24.78	3.6-4.0
7	Azurite	$Cu_2CO_3(OH)_2$	24.85	3.7-3.8
8	Chalcocite	Cu_2S	27.40	5.5-5.8
9	Quartz	SiO_2	11.85	2.6-2.7
10	Hematite	Fe_2O_3	23.56	5.1-5.2
11	Sphalerite	$(Zn, Fe)S_2$	27.18	3.9-4.2
12	Pyrite	FeS_2	22.06	4.9-5.1

Reference Samples for Calibration

Reference samples were prepared for the estimation of reconstruction coefficient for effective atomic number using DE radiography measurements. In this case, aluminum, copper and lead were selected as known materials. These three elements can represent the three different mineral phases usually present in samples from metal mining operations having low attenuation coefficients (gangue, quartz/silicates), medium attenuation coefficients (copper, most base metal minerals) and high attenuation coefficients (molybdenite, galena, lead or other precious metals).

Coefficients k_1, k_2, k_3 and k_4 were then calculated according to Equation 8 using p = 3.8, yielding $k_1 = -8.97 \cdot 10^{11}$, $k_2 = 7.95 \cdot 10^{11}$, $k_3 = 1.88 \cdot 10^{6}$, and $k_4 = -1.16 \cdot 10^{6}$.

Then, the calculated effective atomic number is compared to the actual effective atomic number to determine the accuracy in data correlation and verify calibration, as shown in Figure 4.

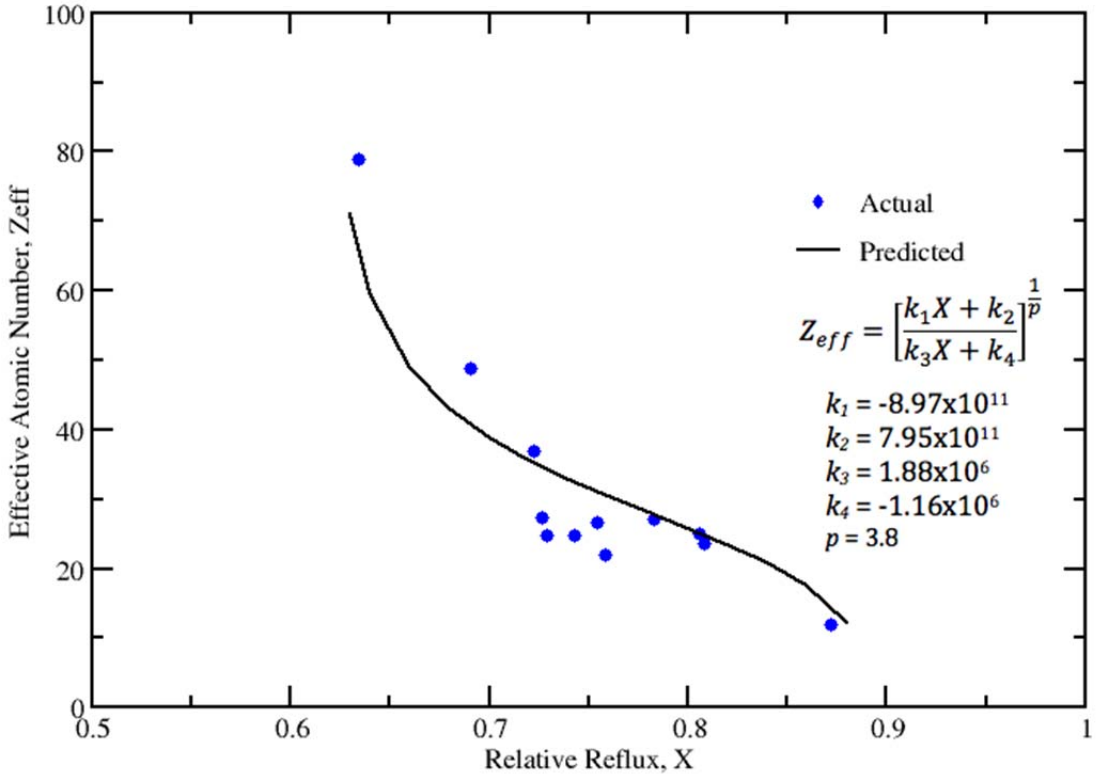

Figure 4. Comparison Between Calculated and Actual Effective Atomic Numbers.

High-Resolution X-Ray Microtomography Calibration

Theory

High-Resolution X-ray Micro Tomography (HRXMT) provides for 3D visualization, characterization, and analysis of multiphase systems at the micron level of voxel resolution. The foundation of HRXMT is to measure the X-ray attenuation of the sample with an appropriate detector. X-ray photons are generated from a point source. Some of the photons are absorbed by the sample, and the attenuated photons are collected on the detector. The intensity measure creates a radiograph, or "projection." The sample absorbs a certain amount of X-ray photons that is determined by the sample density, atomic number, thickness, and linear attenuation coefficient. Different projections are collected when rotating the sample. A collection of projections at different angles in a full rotation can be processed for a three-dimensional reconstruction known as a "backprojection." The sample could be further processed using the reconstructed 3D dataset.

Estimation of Mineral Attenuation Coefficients

It is important to estimate the linear attenuation coefficient before the scan has been taken in order to use the proper settings for the scans. The mass attenuation coefficient has a linear relationship with energy according to Beer's law. Scans for heavy materials with high density and high atomic number require a high-level X-ray energy source in order to get enough X-ray photons to the detector. Therefore, it is very important to determine which level of X-ray energy is sufficient to pass through high-atomic-number and high-density RE samples. The preview of the linear relationship of X-ray mass attenuation coefficient and energy, done using XMuDat software, is shown in Figure 5.

From the estimation of mineral attenuation coefficients, it is evident that the lower the photon energy, the greater the attenuation coefficient difference between minerals. This will make it easier to apply a threshold to radiograph scans and identify only potential RE particles. Additionally, the photon energy should be large enough to pass through the high atomic number and high-density minerals; for example, monazite and zircon. Taking both of those factors into consideration, an energy voltage of 70 kV was selected to scan the samples. Other parameters are defined by considering the projection quality and include an exposure time of 10 seconds for each projection image and a magnification level of 4X.

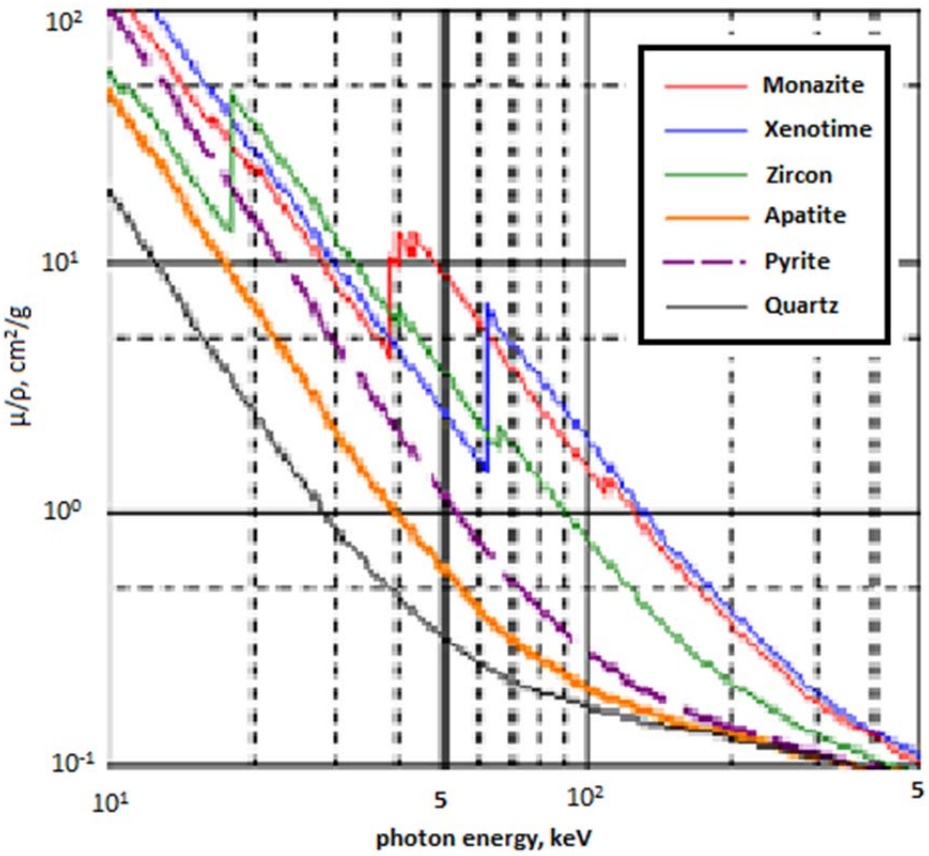

Figure 5. Mineral Attenuation Coefficients Estimated Using XMuDat.

Calibration of Mineral Standards

In order to obtain an accurate analysis of the RE sample, usually the CT standard has to be set for the mineral characterization. Here, from the initial XRD analysis, it is expected that monazite, zircon, apatite and quartz minerals will be present in the samples. Monazite is the mineral of interest as the RE mineral. Therefore, monazite and zircon standards were scanned using the same conditions as the RE sample, which are 4X magnification level, 70 kV energy voltage, and 10 seconds exposure time per projection.

After the reconstruction of CT standards, the CT number distribution map can be exported and transformed into an extension .txt file, which can then be plotted using EXCEL or XMGrace. The CT number distribution map of minerals is shown in Figure 6. From the CT number distribution map of CT standards, it can be seen that monazite has the highest attenuation coefficient and apatite has the lowest. There is a big difference between the high-density and high-atomic-number minerals and gangue mineral apatite. The minerals are clearly distinguished based on their attenuation coefficient. There is some overlap between monazite and zircon, but this is not a serious problem.

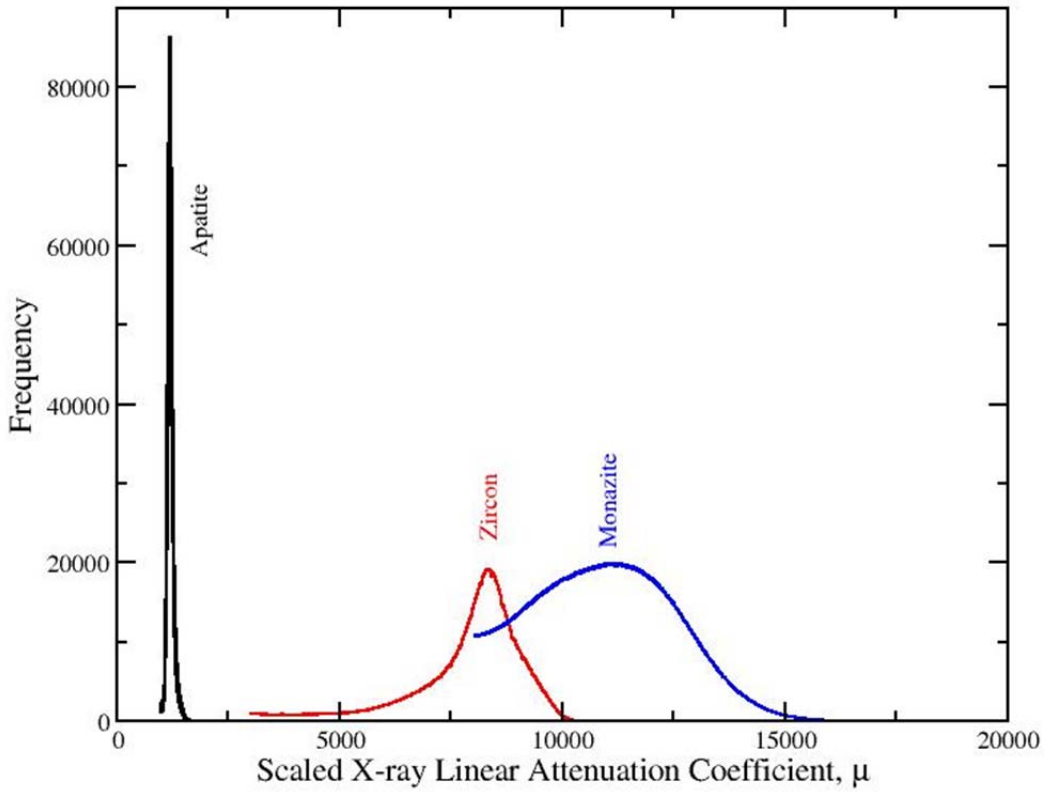

Figure 6. Scaled CT Number Distribution Map for Mineral Phases.

Calibration of Rare Earth Phosphate Sample

Since the CT standards of pure monazite, zircon, and apatite samples have been made, it is possible to generate CT scaled data from the software XMController. This was done for the heavy fraction of the shaking table concentrate after scanning, and the reconstruction with scaled data using the standards can be seen in Figure 2. The same scaling was applied to the HRXMT samples of this project.

TASK 3: DUAL-ENERGY (DE) RADIOGRAPHY

In order to begin the DE radiography scans, a vibrating riffler was used to separate out a representative portion from each size class of each sample and the subsample was attached to a slide (glass plate) using double-sided sticky tape and secured using a second slide. Three slides were prepared from each size class for each sample, making a total of nine slides per sample and 27 slides in total. Each slide has roughly 34,000 particles attached to it, so a total of 102,000 particles from each size class for each sample were then imaged.

The DE radiography scans were completed by splitting the slide into 40 sections, making a 4 × 10 grid, and scanning each section at a low energy level (80 kV) and a high energy level (140 kV).

The attenuation coefficients recorded from the DE radiography were used to find the relative reflex, *R*, which then gave an effective atomic number using the calibration curve completed in Task 2. To do this, Matlab was utilized to read each radiograph at both high and low energies and compare the two scans, which gave the relative reflex (*X*) pixel by pixel. Once the relative reflex was calculated, a threshold was applied to identify the potential rare earth (RE) particles. Thresholding discards all the relative reflex values above a given point and accepts those below it. The threshold number used was $X = 0.70$, which corresponds to $Z_{eff} = 38$. This means that all of the values where $X < 0.70$ were accepted, giving particles with $Z_{eff} > 38$. This threshold was chosen based on the calibration curve (see Figure 4 in Task 2), and tested on a sample of pure bastnasite, seen in Figure 7.

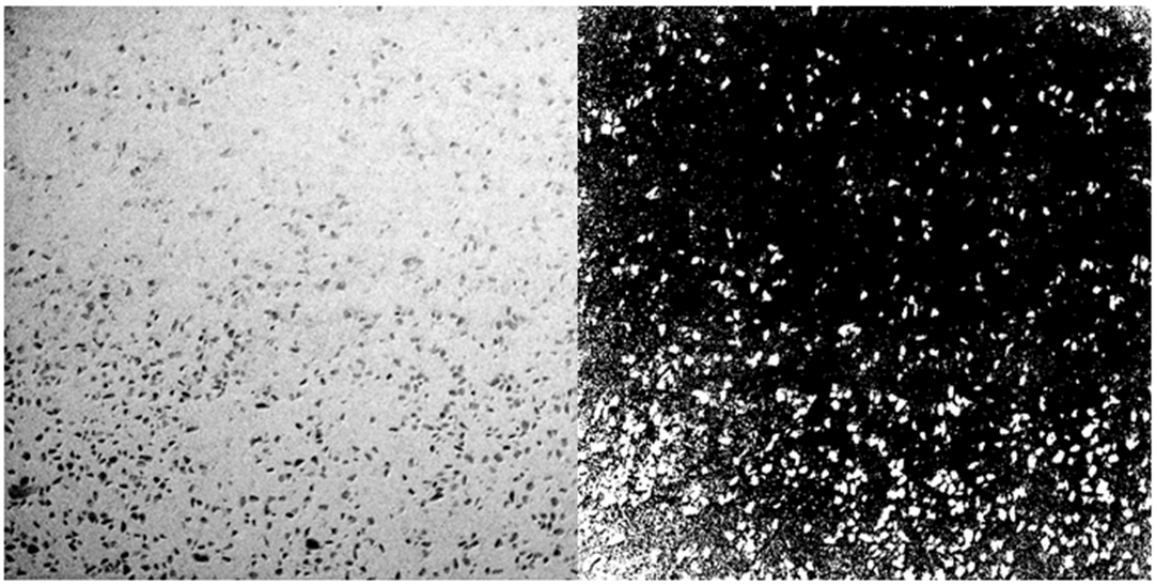

(a) (b)

Figure 7. Bastnasite (a) Radiograph and (b) Resulting Thresholded Image Used for Threshold Verification.

Looking at the calibration curve, 0.70 might seem a little high when looking for RE particles. However, as the particle density increases, the 80 kV and 140 kV energies that were used might have some difficulties penetrating the particles. Due to this effect, the accuracy of the calibration curve as it nears higher atomic numbers decreases. Therefore, 0.70 was utilized to make sure all the potential RE particles were gathered. Examples of the DE radiography scans taken at high and low energies, their corresponding relative reflex image, and the image after thresholding can be seen in Figures 8, 9, and 10. Note that the dark particles in the DE scans correspond to the white portions in the thresholded images and are potential RE particles.

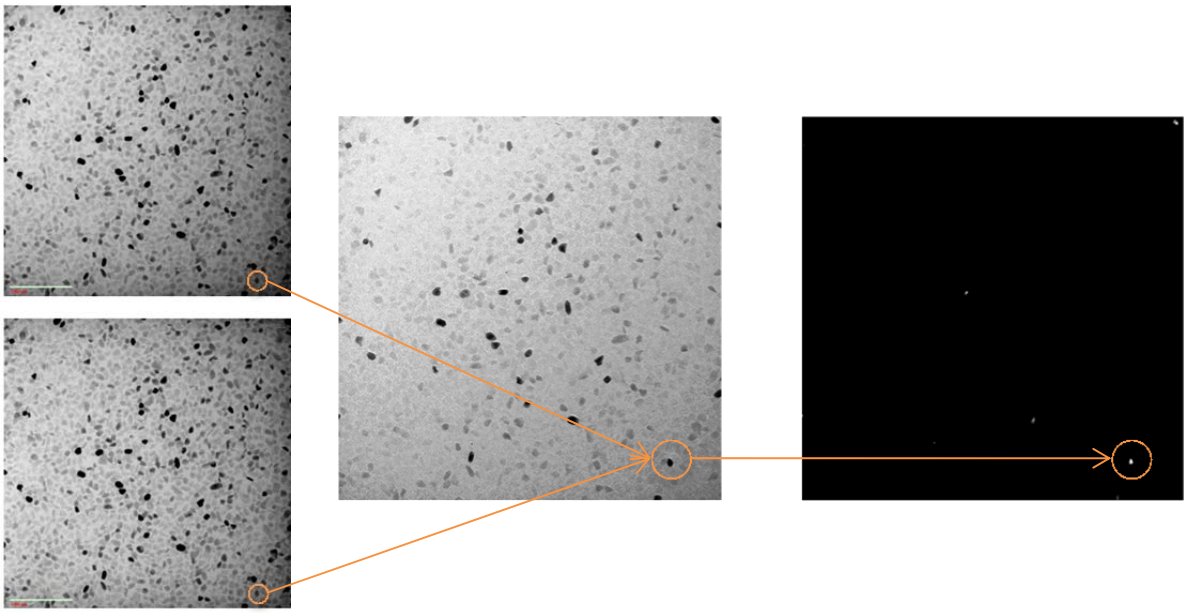

Figure 8. DE Scans, Relative Reflex, and Thresholded Image of a Section from Shaking Table Concentrate.

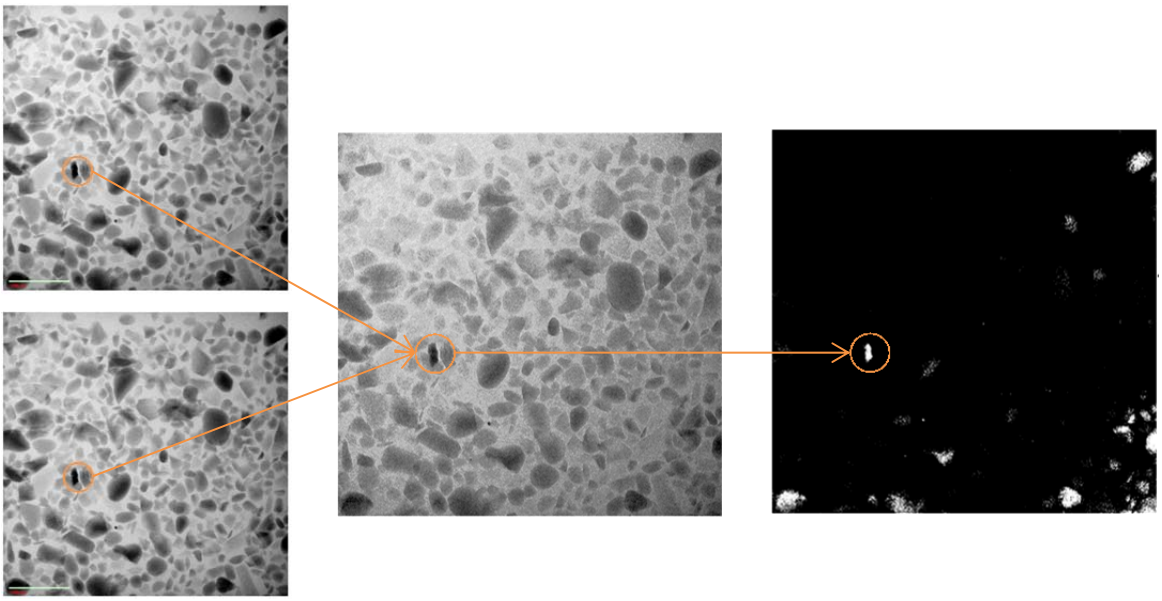

Figure 9. DE Scans, Relative Reflex, and Thresholded Image of a Section from Acid Plant Feed.

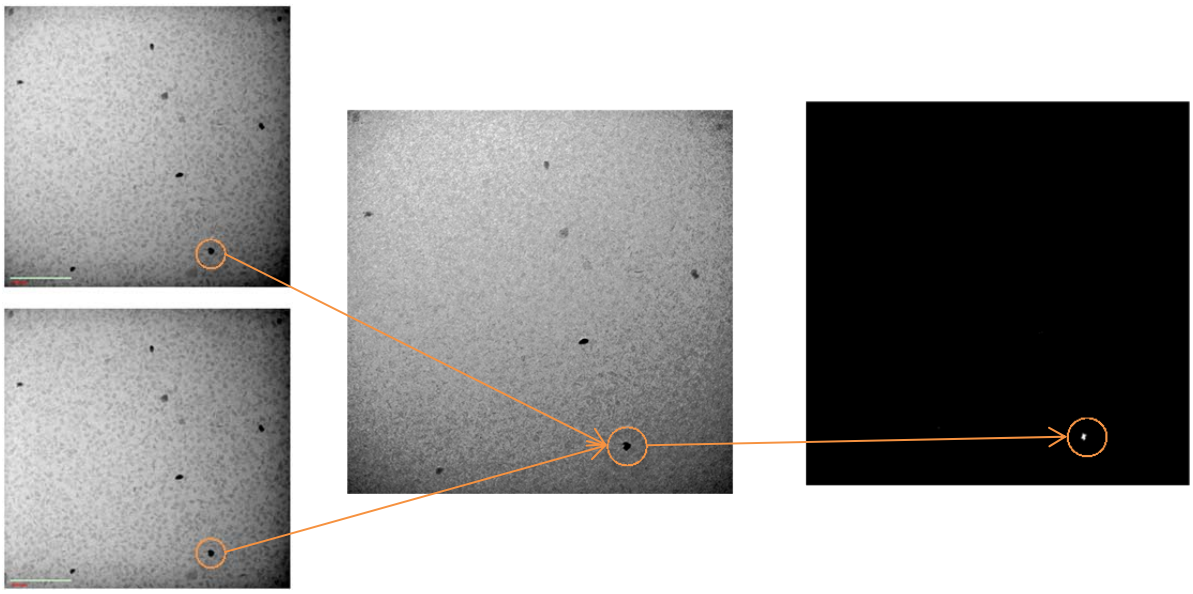

Figure 10. DE Scans, Relative Reflex, and Thresholded Image of a Section from Phosphogypsum.

While some of these thresholded images appear to have a good number of potential rare earth particles, it is important to remember that each image is only one of 120 possible images for each size group of each sample, and the majority of the other images have no potential particles shown.

TASK 4: HIGH-RESOLUTION X-RAY MICROTOMOGRAPHY (HRXMT)

The particles that were identified and isolated using DE radiography were removed and prepared for the HRXMT scanning. For this portion of the test, the samples were secured in a plastic cylindrical tube. Samples from different slides were separated by a circular paper, as can be seen in Figure 11. The final prepared samples can be seen in Figure 12.

The samples were then scanned using the conditions determined in Task 2; that is, 70 kV energy and 10 seconds per image. One thousand projection images were taken while rotating the samples 360°. This created a series of projection images, several of which can be seen in Figure 13, which were then used to reconstruct a 3D digital copy of each sample using the phosphate rare earth standard created and used in Task 2 for calibration. These can be seen in the Results section of this report.

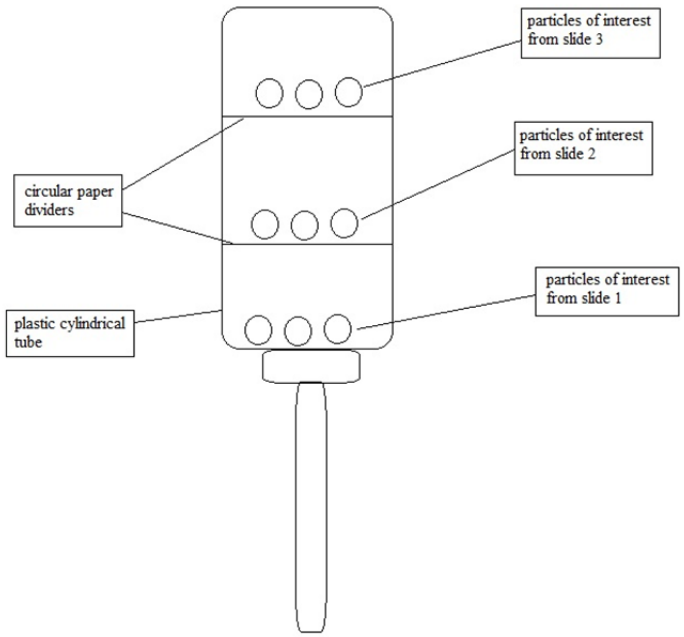

Figure 11. Sample Preparation Setup for HRXMT Scanning.

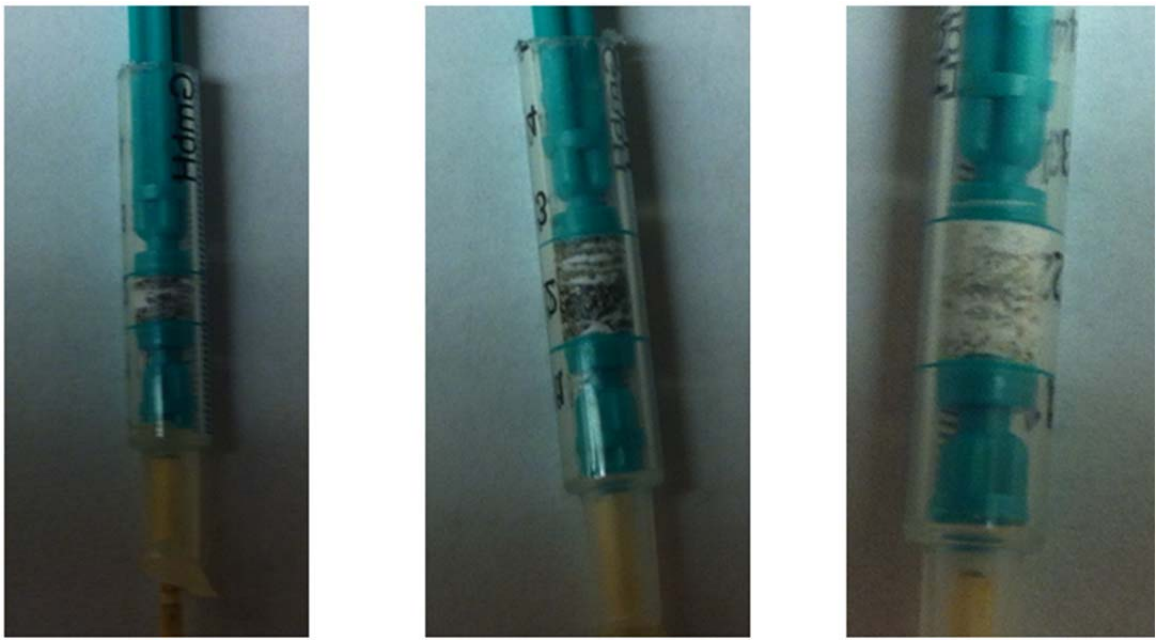

(a) (b) (c)

Figure 12. Final HRXMT Samples for (a) Shaking Table Concentrate, (b) Acid Plant Feed, and (c) Phosphogypsum.

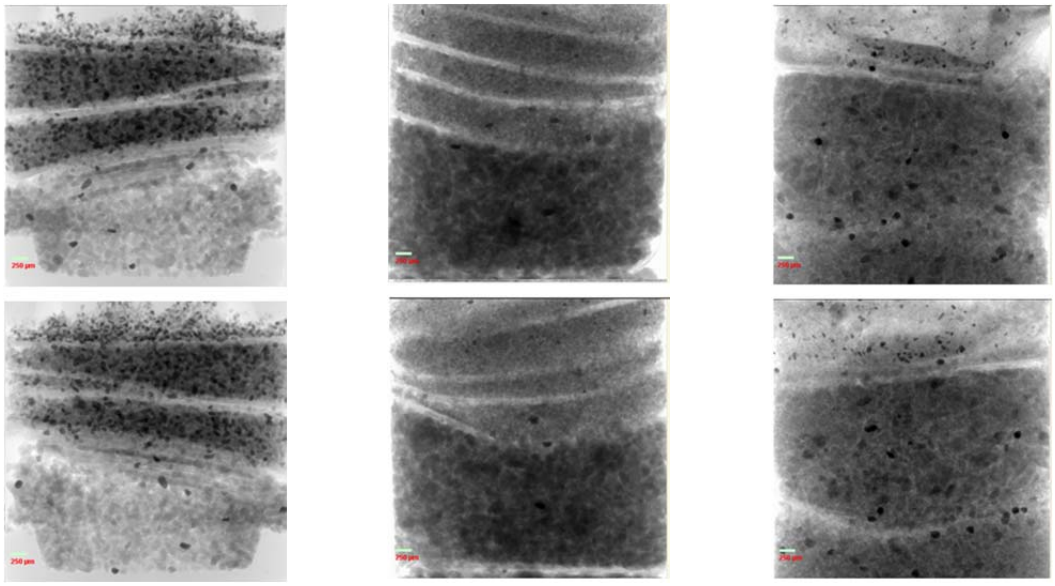

(a) (b) (c)

Figure 13. Projection Images from (a) Shaking Table Concentrate, (b) Acid Plant Feed, and (c) Phosphogypsum before Reconstruction.

RESULTS

DE RADIOGRAPHY RESULTS

Out of the 27 slides scanned using DE radiography, 11 slides had no potential RE particles after thresholding. The number of sections removed from each slide and which slides contained potential RE particles can be seen in Table 4.

Table 4. Number of Sections with Potential RE Particles on Each Slide.

Sample Stream	Size Range	Slide Number	Number of Sections with Potential RE Particles
Shaking table concentrate	>106 μm	2	3
Shaking table concentrate	>106 μm	3	3
Shaking table concentrate	75-106 μm	11	8
Shaking table concentrate	75-106 μm	13	5
Shaking table concentrate	53-75 μm	22	1
Acid plant feed	>106 μm	32	2
Acid plant feed	>106 μm	33	8
Acid plant feed	75-106 μm	41	8
Acid plant feed	75-106 μm	42	6
Acid plant feed	75-106 μm	43	3
Acid plant feed	53-75 μm	53	10
Phosphogypsum	>106 μm	61	11
Phosphogypsum	>106 μm	62	14
Phosphogypsum	75-106 μm	71	1
Phosphogypsum	75-106 μm	72	7
Phosphogypsum	53-75 μm	82	12

Note that for shaking table concentrate and acid plant feed, the majority of the sections contain particles in the size range of 75-106 μm and only a small amount of particles are in the size class of 53-75 μm, and that the phosphogypsum had the most particles come from the size range of >106 μm and the least amount from the 75-106 μm range. This is important for the possible size range and liberation analysis for RE particles in those sample streams.

HRXMT SCAN RESULTS

The 3D digital samples can be viewed as 2D slices, as seen in Figure 14, or as full 3D renderings, as in Figure 15. Using a digital viewing program, Drishti, the 3D images can be thresholded to view their individual mineral breakdown, pictured in Figures 16, 17, and 18. When imported to ImageJ, the number of particles past a certain threshold can be counted to get an accurate concentration.

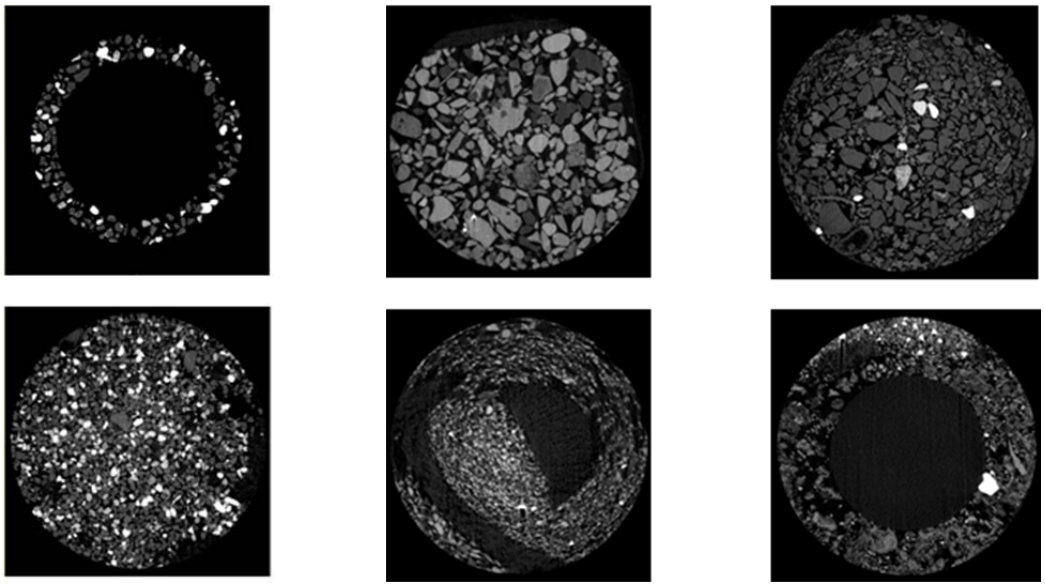

Figure 14. 2D Slice from (a) Shaking Table Concentrate, (b) Acid Plant Feed, and (c) Phosphogypsum after Reconstruction.

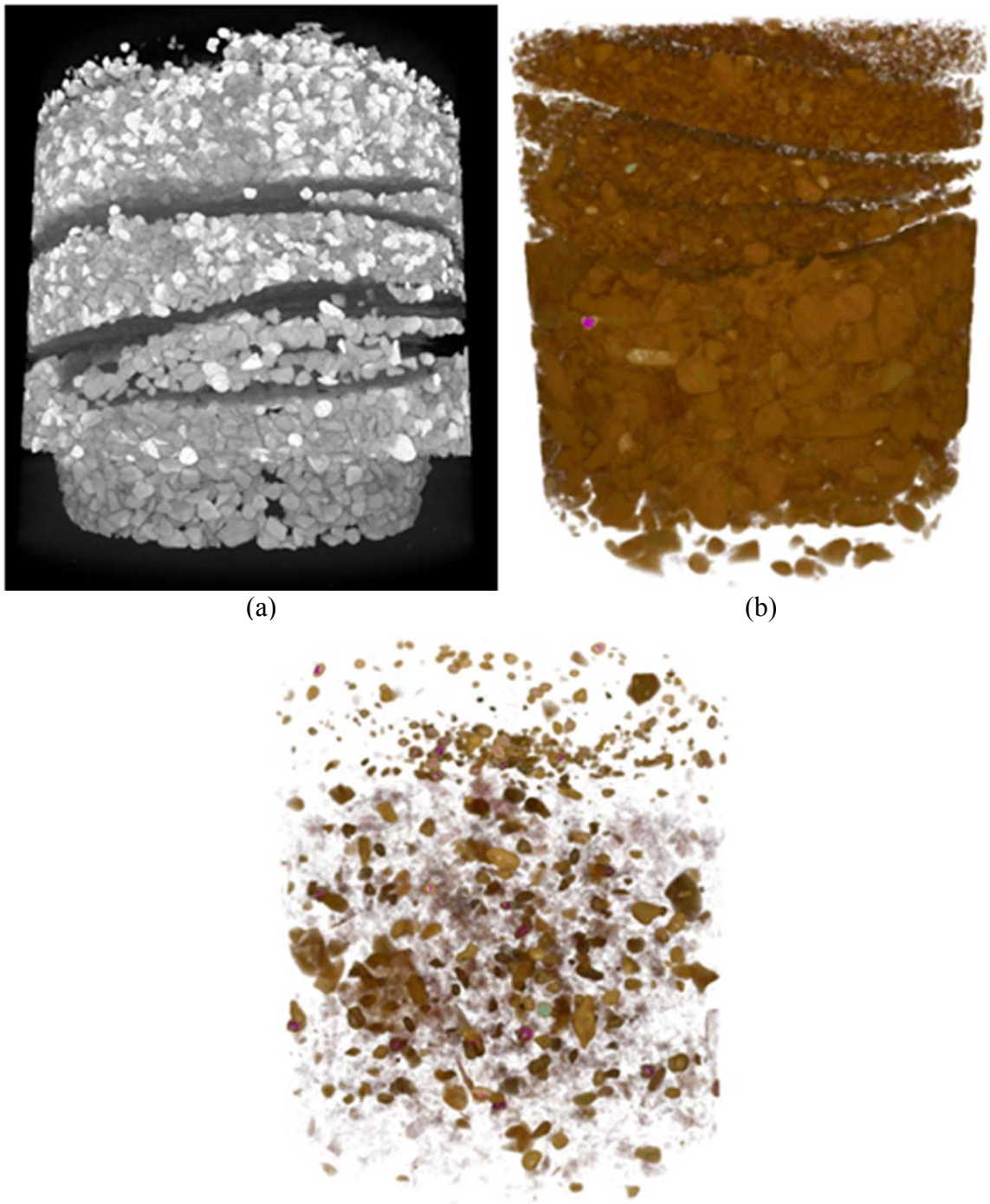

Figure 15. 3D Reconstruction of (a) Shaking Table Concentrate, (b) Acid Plant Feed, and (c) Phosphogypsum.

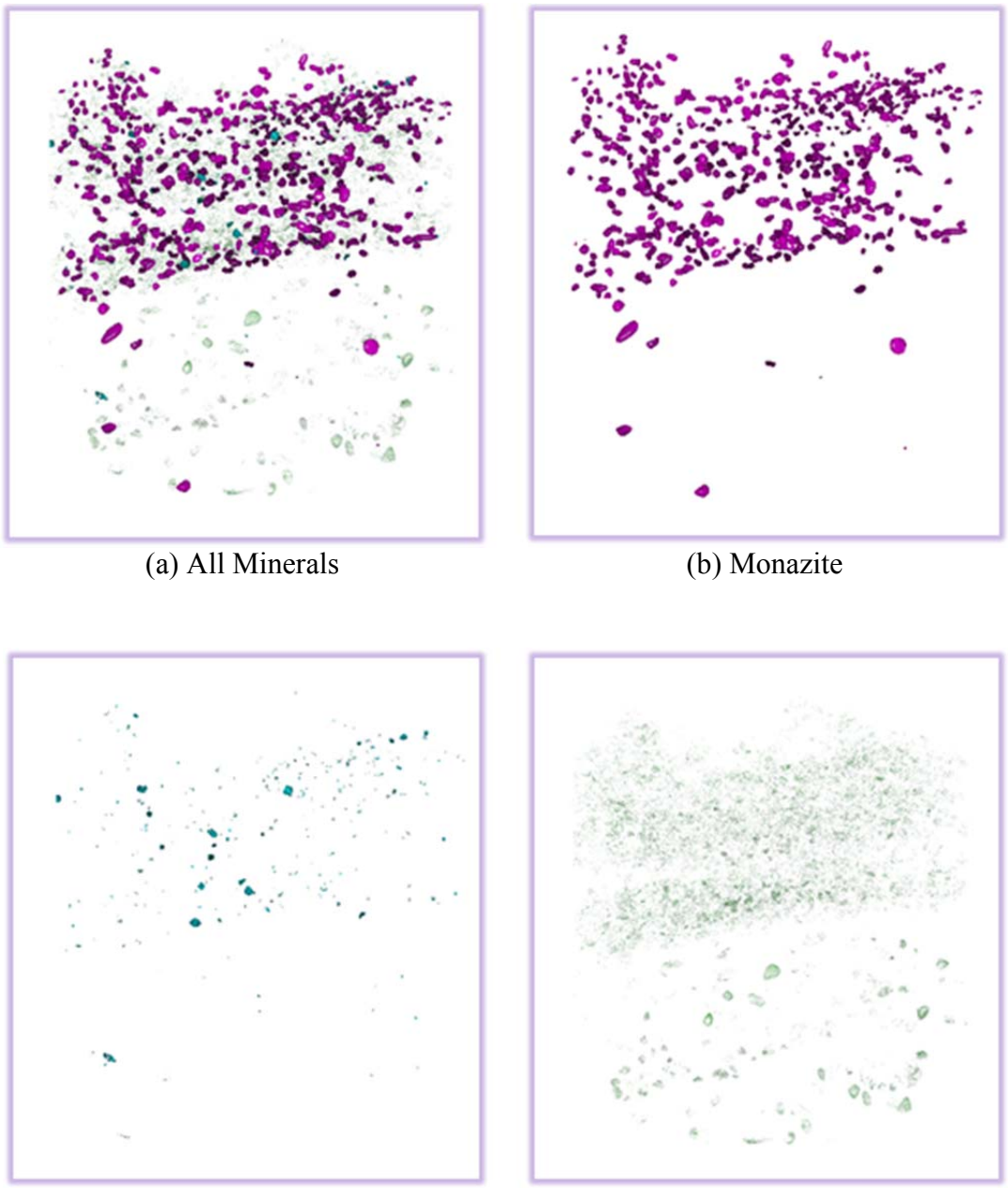

(a) All Minerals (b) Monazite

(c) Zircon (d) Apatite

Figure 16. Shaking Table Concentrate 3D Reconstruction by Mineral Composition.

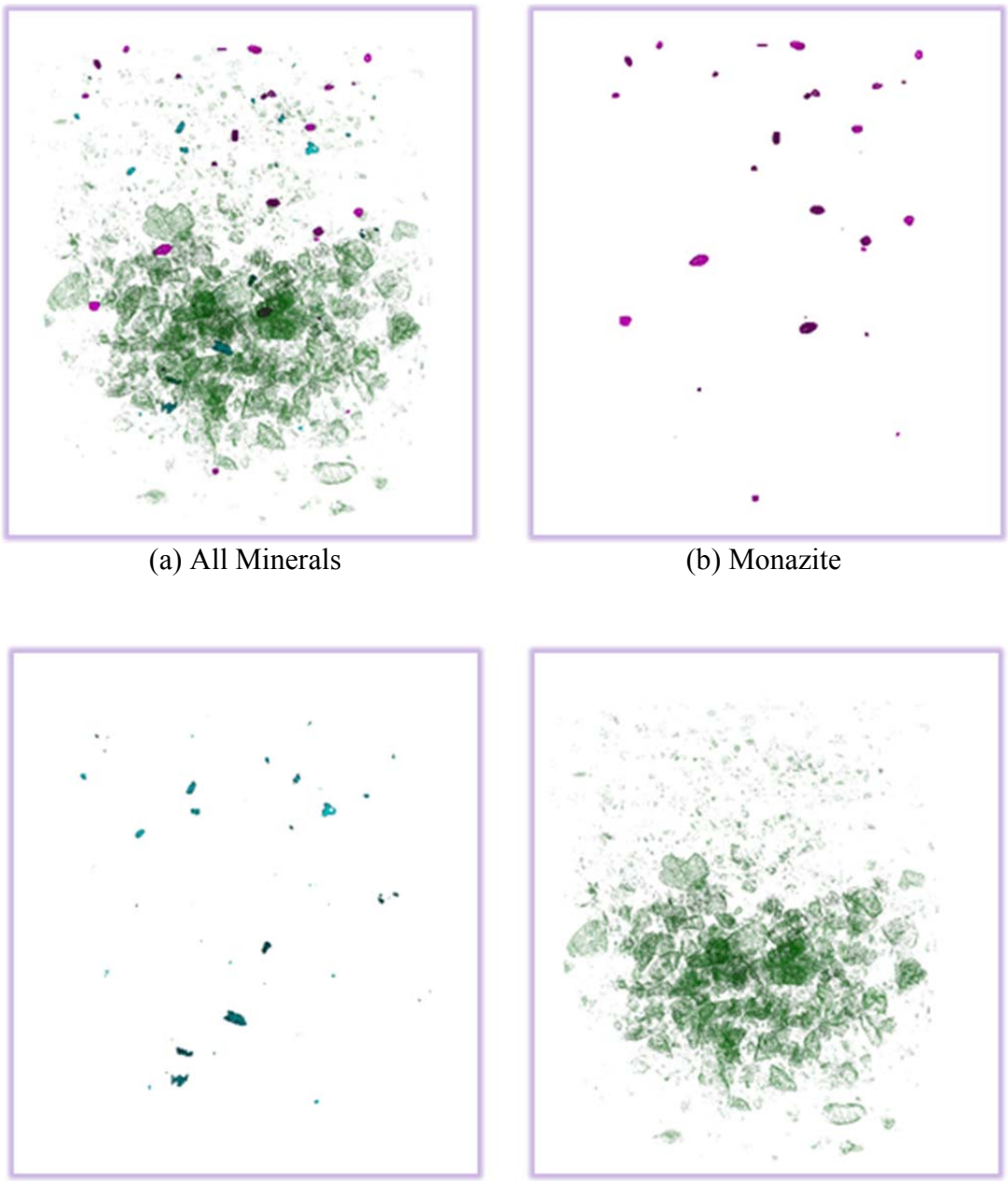

(a) All Minerals (b) Monazite

(c) Zircon (d) Apatite

Figure 17. Acid Plant Feed 3D Reconstruction by Mineral Composition.

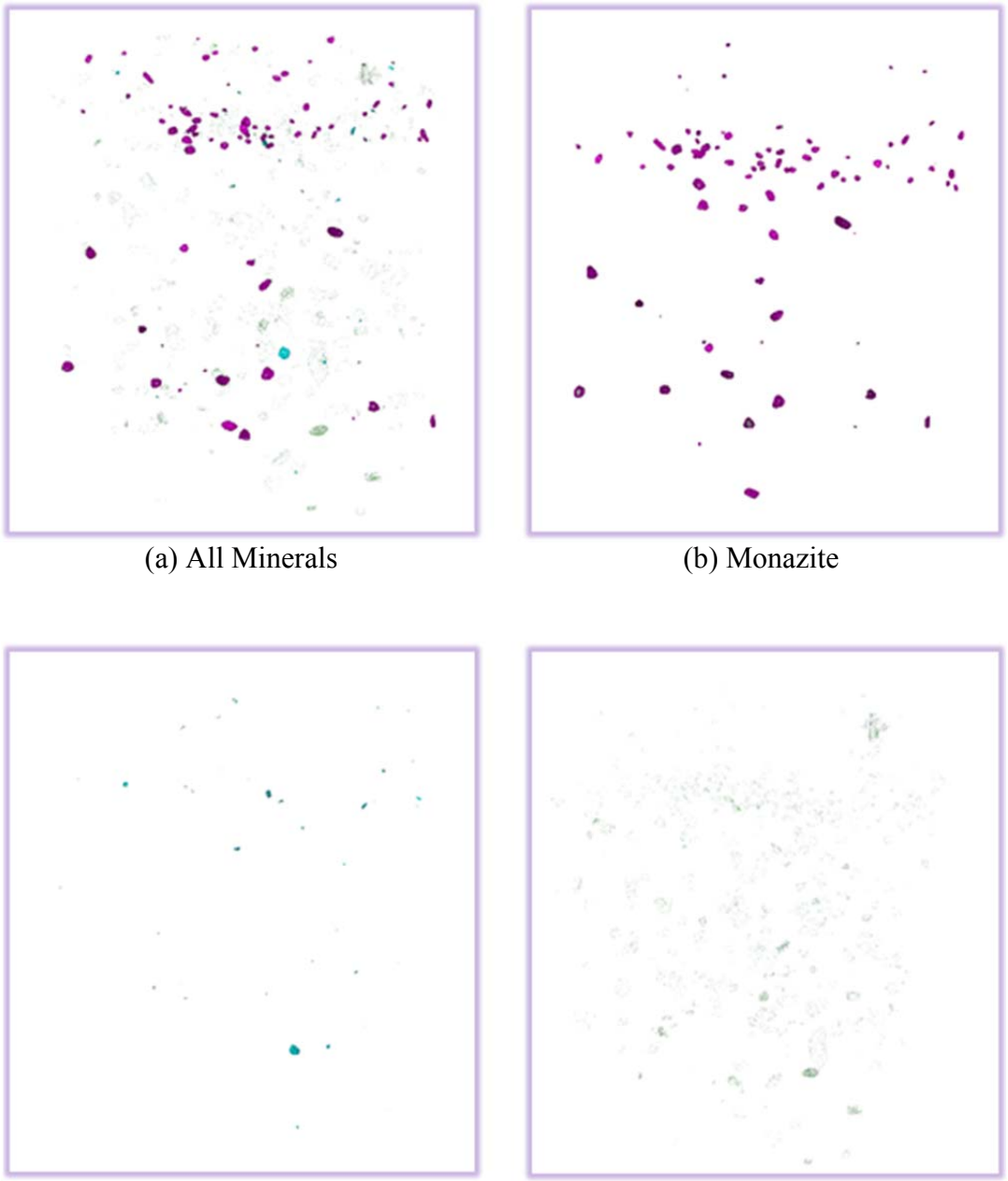

(a) All Minerals (b) Monazite

(c) Zircon (d) Apatite

Figure 18. Phosphogypsum 3D Reconstruction by Mineral Composition.

PARTICLE ANALYSIS FROM HRXMT

The final mineral count per sample after reconstruction was found using the 3D Object Counter plugin through ImageJ and using the thresholding values per mineral found in Figure 6 of Task 2. The final mineral count can be found in Table 5.

Table 5. Final Monazite Count Per Sample.

Sample	Number of RE Particles	RE Particle Concentration (ppm)
Shaking table concentrate	660	2157
Acid plant feed	32	104
Phosphogypsum	87	284

During the final thresholding of the particles, there was some inevitable overlap between the monazite CT numbers and the zircon CT numbers, as shown in Figure 6. There could be some error in the particles identified as monazite. Per sample, 18 particles from the shaking table concentrate, 5 particles from the acid plant feed, and 7 particles from the phosphogypsum belong to this somewhat nebulous zone. However, as these are at the very edge of the zircon identification zone, where the CT number is between 9000 and 10000, it was ultimately decided that these particles are most likely monazite and so they were counted in the RE particle category. Of those identified as zircon, 164 particles from the shaking table concentrate, 26 particles from the acid plant feed, and 28 particles from the phosphogypsum also belong to the region belonging to both monazite and zircon. However, as the CT numbers in this range, between 8000 and 9000, are closer to the peak of zircon and only belong to the edge of monazite, the particles can be reasonably identified as zircon and not monazite. Therefore, the ppm count shown in Table 5 can be reasonably concluded to be accurate.

Using ImageJ, a visual examination of each sample can determine the degree of liberation of the monazite particles. Because the DE slides were separated in the HRXMT samples by paper, it is possible to look at each size class individually to examine the degree of liberation for each size class of each sample. For the shaking table concentrate, the monazite particles in all three size classes are fully liberated. Additionally, reexamining the mineral breakdown by approximate size classes, found in Figures 19, 20, and 21, notice that in the shaking table concentrate the majority of the monazite is found at the top of the sample. All three HRXMT samples were prepared so that the largest particles were found at the bottom and the smallest at the top. However, because the shaking table concentrate only contained one section of one slide in the size range of 53-75 μm, most of these particles near the top of the sample were located on the slides with the particle size range of 75-106 μm. This means that the majority of the monazite particles can be found in this size range and fully liberated, making it the optimum size for grinding and processing.

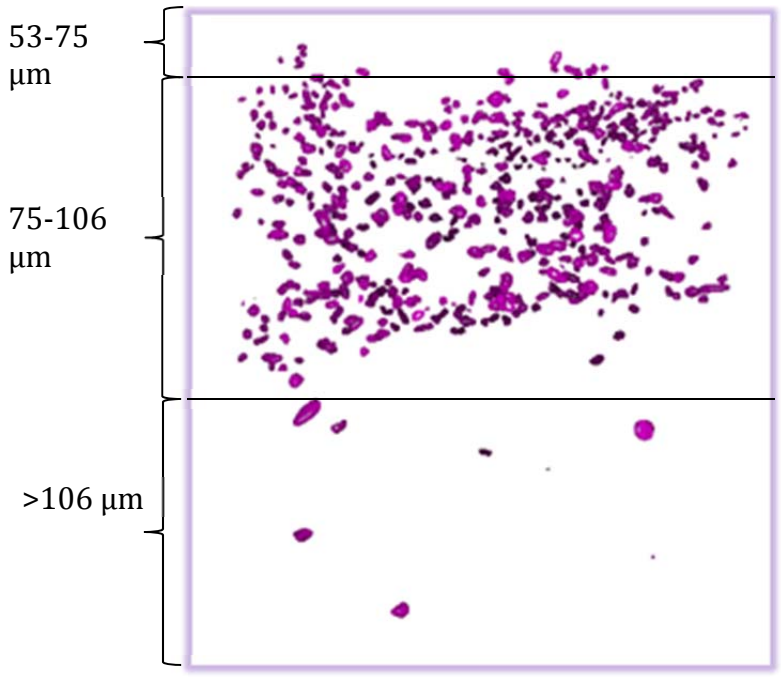

Figure 19. Monazite in 3D Reconstruction of Shaking Table Concentrate Separated Approximately by Size Class.

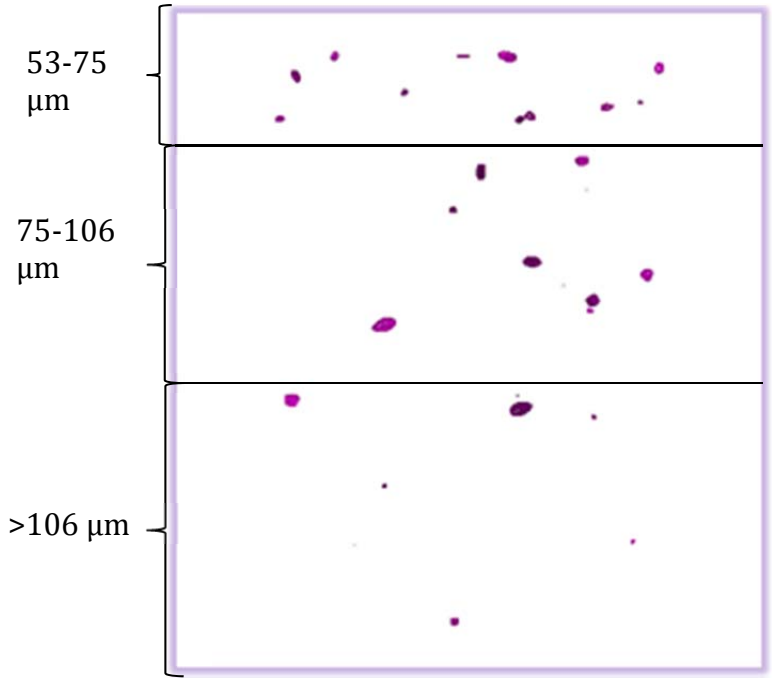

Figure 20. Monazite in 3D Reconstruction of Acid Plant Feed Separated Approximately by Size Class.

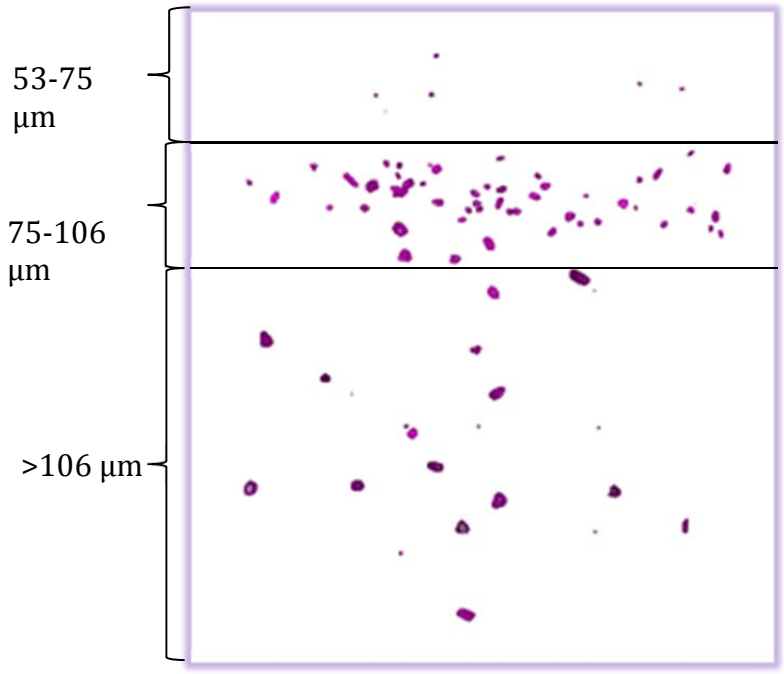

Figure 21. Monazite in 3D Reconstruction of Phosphogypsum Separated Approximately by Size Class.

The phosphogypsum is liberated to a similar degree. In the size range of >106 µm, the majority of the monazite particles are fully liberated, though with a few particles that are partially locked, making about a 95% degree of liberation. For the size classes of 75-106 µm and 53-75 µm, all the monazite particles are fully liberated. The phosphogypsum sample (Figure 21) has a similar grouping as the shaking table concentrate further from the top of the sample, where particles from the 75-106 µm range were located as well. However, there are many particles grouped together throughout the rest of this sample as well, especially in the >106 µm range. Because the majority of the RE particles are liberated as well, the optimum size range cannot be stated as clearly as the shaking table concentrate, but should be in the approximate range of 75-106 µm, although a larger size could reasonably be considered.

The liberation analysis of the acid plant feed was a bit different from the other two samples. For the size class of >106 µm, the majority of the monazite particles are not liberated at all. In fact, the RE particles are about 95% fully locked. An example of this can be seen in the 2D slice of the sample shown in Figure 22. However, in the smaller size ranges, the monazite is nearly fully liberated. Like the other two samples, only a small amount of the HRXMT sample came from the size range of 53-75 µm, therefore making this size range not ideal for grinding, even though monazite particles in this size range are fully liberated. The acid plant feed (Figure 20) has a much lower concentration of monazite than the other two samples and it is concentrated relatively uniformly throughout the sample and throughout the size groups. Because the particles >106 µm are not liberated, but not many particles from 53-75 µm were potential RE

minerals, the size class of 75-106 µm should be considered as a good size range for monazite retrieval.

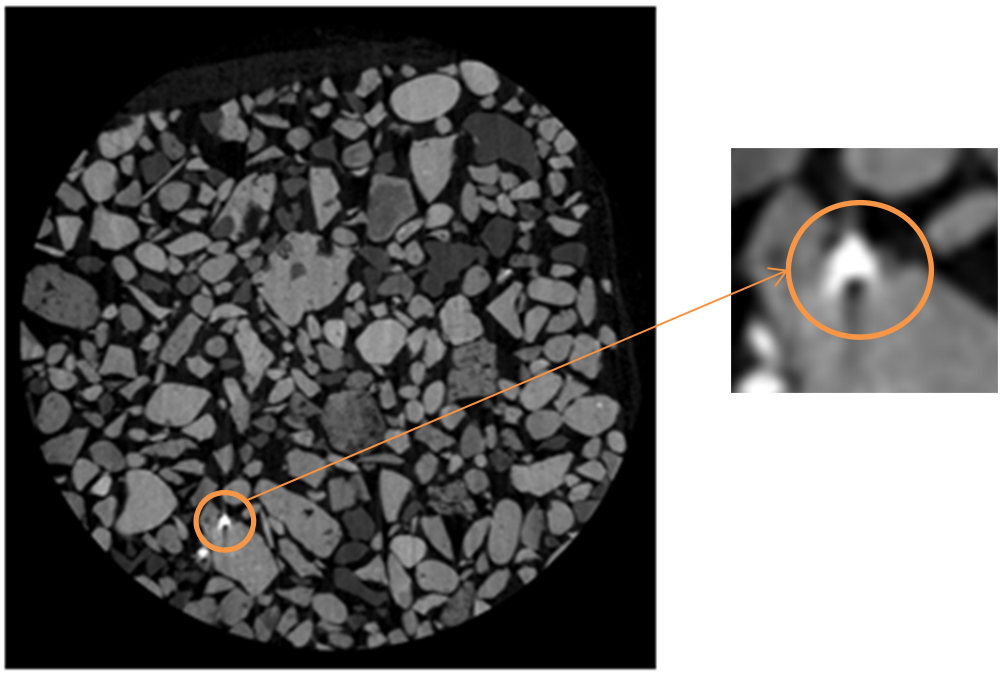

Figure 22. A Locked Particle of Acid Plant Feed Found in the Size Class of >106 µm.

CONCLUSIONS AND RECOMMENDATIONS

Using DE radiography and HRXMT, the concentrations of RE minerals in the samples provided were as follows: 2157 ppm in the shaking table concentrate, 104 ppm in the acid plant feed, and 284 ppm in the phosphogypsum. Judging from the degree of liberation for each sample and size range, the best particle size range to find fully liberated monazite particles is 75-106 μm, although other sizes can reasonably considered for acid plant feed and phosphogypsum.

While the concentrations follow the trend from the chemical analysis, meaning that the shaking table concentrate has a higher concentration than the acid plant feed, the concentration for the acid plant feed is much lower than anticipated. Part of this error can be explained due to a portion of all the samples, the particles that were <53 μm not being included in the analysis. However, some error could be caused by RE particles not being identified on the DE slides and so were not transferred to the HRXMT sample. For this to happen, there could have been a manual error in the physical process of removing the particles or an error due to an incorrect thresholding value. The lower than expected concentration could be caused by any of the three described scenarios or all three possibilities compounded.

From these results, it can be concluded that DE radiography followed by HRXMT scanning is an effective and efficient method for resource identification, particularly for RE mineral identification. Based on the accuracy of DE radiography correctly identifying potential RE particles, DE radiography could even be used solely to identify RE particles given a machine that can produce X-rays at a sufficiently high energy level. Because of the amount of information this method of resource identification can provide about the individual particles in each sample, in addition to the level of accuracy HRXMT has due to its three-dimensional nature, it is recommended that DE radiography be used to semi-quantitatively identify minerals of interest followed by a thorough particle analysis from HRXMT scanning and reconstruction in order to isolate and characterize RE particles.

The main limitation of this method is the amount of time required for HRXMT scanning. This is reduced by using DE radiography to “pre-concentrate” the HRXMT samples with particles more likely to be RE minerals, but the time still required to scan enough particles to gain a reliable accuracy is not insignificant. However, if an X-ray source could produce X-rays of high enough energy level, identification confirmation by HRXMT would not be a necessary follow-up to DE radiography. RE particle identification could be done in a matter of minutes instead of hours or days. In this sense, the project is further limited by the maximum energy level the X-ray machine can produce. As demonstrated by previous literature (Lin and others 2013), the maximum effective atomic number that can be accurately identified using solely DE radiography with the machine used in this project is an atomic number of 40, thus HRXMT verification is necessary.

Despite these limitations, this project has demonstrated that DE radiography followed by HRXMT is still a more effective method for particle identification and liberation analysis than other methods available. Using DE radiography first reduces the time necessary for just HRXMT scanning and using HRXMT for particle verification compensates for insufficient energy levels during DE radiography. It is recommended that this method be used in the future for RE identification and analysis.

REFERENCES

Humphries M. 2013. Rare earth elements: the global supply chain. Washington: Congressional Research Service. CRS Report R41347.

Lin CL, Hsieh C-H, Tserendagva T-A, Miller JD. 2013. Dual energy rapid scan radiography for geometallurgy evaluation and isolation of trace mineral particles. Minerals Engineering 40: 30-7.

Naydenov SV, Ryzhikov VD, Smith CF. 2003. Direct reconstruction of the effective atomic number of materials by the method of multi-energy radiography. Nuclear Instruments and Methods in Physics Research B 215: 552-60.

Zhang P. 2012. Recovery of critical elements from Florida phosphate: Phase I. Characterization of rare earths. Presented at: Engineering Conferences International (ECI), Rare Earth Minerals/Metals Sustainable Technologies for the Future; 2012 August 12-17; San Diego, CA. Unpublished.